Geomorphology 466 (2024) 109409

Contents lists available at ScienceDirect

Geomorphology

journal homepage: www.journals.elsevier.com/geomorphology

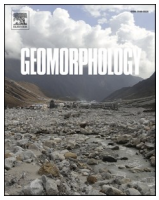

Shore ice control on coastal geomorphic evolution in cold regions

E.J. Theuerkauf [a,*], L.K. Zoet [b], C.A. Volpano [b], S.E. Dodge [b], B.M. Hartley [a], J. Elmo Rawling III [c]

[a] Department of Geography, Environment, and Spatial Sciences, Michigan State University, 673 Auditorium Road, East Lansing, MI 48824, United States of America
[b] Department of Geoscience, University of Wisconsin-Madison, 1215 West Dayton Street, Madison, WI 53706, United States of America
[c] Wisconsin Geological and Natural History Survey, University of Wisconsin-Madison, 3817 Mineral Point Road, Madison, WI 53705, United States of America

ARTICLE INFO

Keywords:
Shore ice
Coastal erosion
Geomorphology
Sediment transport
Cold regions
Wave tank

ABSTRACT

Shore ice is a common feature on cold climate coasts, which are abundant in mid- and high-latitude regions, however it is understudied. Previous research has reported both beach protection and erosion as potential impacts from shore ice presence. Altered ice dynamics resulting from a changing climate are likely to intensify these impacts. To address this discrepancy and improve future coastal change predictions we conducted the first combined field, laboratory and modeling study of shore-ice processes and impacts. Beach and nearshore morphology mapping, experiments with a novel cryogenic wave tank, and 3D coastal evolution modeling revealed that shore ice protected the beach from storms, but scoured the nearshore at the ice edge and transported sediment offshore, likely past the depth of closure. This resulted in enhanced beach erosion during the ice-free and non-storm season, countering the protective benefit from the ice. This study indicates that shore ice plays an important and likely evolving role in geomorphic evolution along cold climate coasts.

1. Introduction

Cold climate coastlines are important from economic and ecological perspectives yet are vulnerable landscapes (Zimmermann et al., 2022). The presence of ice in these environments plays an important role in regulating biological and geomorphic processes and has cultural significance (Brady and Leichenko, 2020). The band of ice immediately along the coast in these regions is referred to as shore ice (sometime referred to as shorefast ice). Shore ice is typically considered a protective buffer to the portions of the coast landward of the shoreline, such as beaches and permafrost terrains (Barnes et al., 1993; Forbes and Taylor, 1994), however, some studies report that the presence of ice can enhance coastal erosion due to offshore rafting of material during ice breakup or seabed scour immediately adjacent to the ice front (Barnes et al., 1994; Kempema et al., 2001). These conflicting models on the geomorphic role of shore ice presents a challenge for understanding and managing cold climate coastlines, as the presence or absence of shore ice is clearly an important factor for coastal erosion vulnerability. Shortened winter shore ice seasons, decreased ice concentrations, and increased shore ice variability (e.g., sub-Arctic and northern temperate) are all expected over the next century in cold climate areas (Brady and Leichenko, 2020; Zimmermann et al., 2022). Evaluating the role of shore ice in coastal change is becoming increasingly important given its changing dynamics in response to climate change.

The presence of the nearshore ice complex (NIC) is commonly thought to protect beaches and dunes from the erosive power of winter storm waves (Bryan and Marcus, 1972; Marsh et al., 1973; Evenson and Cohn, 1979; Miner and Powell, 1991; Manson et al., 2015). Previous studies have reported both lower shoreline erosion rates during years with shore ice present (BaMasoud and Byrne, 2012), and high magnitude erosion resulting from winter storms that occur in the absence of shore ice (Theuerkauf et al., 2021). The fundamental mechanism by which shore ice can protect the beach from erosion is through the development of the NIC (Fig. 1). As cold conditions persist during the winter the NIC will evolve from an icefoot that initiates on the beach (Evenson and Cohn, 1979; Dodge et al., 2022). If calm wave conditions prevail the ice will begin to grow basinward from the icefoot forming an ice lagoon (Barnes et al., 1993; Theuerkauf et al., 2023). If wavy conditions occur, the NIC can grow quickly basinward as available brash and slush ice is pushed landward during storms (Bryan and Marcus, 1972; Marsh et al., 1973). Ridges of ice are formed as brash and slush ice is shoved against or thrown upon the icefoot or ice lagoon. Generally, these ridges form in association with the nearshore bar and trough system as this is the zone where wave breaking and associated brash and slush ice transport occurs (Bajorunas and Duane, 1967; Bryan and Marcus, 1972; Seibel et al., 1976; Barnes et al., 1994). Wavy conditions

* Corresponding author.
E-mail address: theuerk5@msu.edu (E.J. Theuerkauf).

https://doi.org/10.1016/j.geomorph.2024.109409
Received 4 March 2024; Received in revised form 9 August 2024; Accepted 26 August 2024
Available online 7 September 2024

can also result in NIC destruction depending on the magnitude and direction of wave energy, ambient air and water temperature, and supply of brash and slush ice (Bryan and Marcus, 1972; Marsh et al., 1973; McCann and Taylor, 1975; Miner and Powell, 1991; Barnes et al., 1994; Theuerkauf et al., 2023). The cycle of NIC growth, stability, and decay may occur multiple times throughout a winter season resulting in temporal variability in the amount of beach and nearshore protection from wave erosion (Miner and Powell, 1991).

While a lack of shore ice can clearly lead to enhanced coastal erosion during winter storms, previous research has indicated that shore ice itself may have an erosive impact, particularly on the nearshore bed (Bajorunas and Duane, 1967; Marsh et al., 1973). Erosion associated with shore ice is primarily induced when ice breaks apart during wave events or at the end of the ice season (Seibel et al., 1976; Miner and Powell, 1991; Dodge et al., 2022). When breakup occurs chunks of sediment laden ice can collide with the beach or seabed resulting in scour (Barnes et al., 1994). Perhaps more importantly, this sediment-laden ice can then be rafted into deeper water if offshore winds occur, effectively removing the material from the nearshore sediment budget (Barnes et al., 1994; Kempema et al., 2001; Dodge et al., 2022). An additional mode of nearshore erosion has been documented in some studies related to wave scour immediately basinward of the NIC (Barnes et al., 1994). Previous work has indicated that as waves interact with the basinward edge of the ice, the energy is directed downward towards the seabed, resulting in scour (Barnes et al., 1993; Bajorunas and Duane, 1967). The dynamics of this process have been likened to the impacts of a seawall on nearshore bathymetry, however no studies to-date have been able to document the exact spatial and temporal extent of this scour or where the scoured sediment might be transported.

With climate change, cold-coast regions are likely to experience changes in the shore ice regime that could enhance the erosive impacts (Brady and Leichenko, 2020; Zimmermann et al., 2022). The most obvious impact would be reduced presence of shore ice and the increased exposure of beaches to storm waves. A decrease in shore ice has been documented in cold-coast regions including the Great Lakes of North America (Wang et al., 2018) and the Arctic (Forbes and Taylor, 1994; Brady and Leichenko, 2020; Zimmermann et al., 2022). With climate change, the ice season is expected to be shortened with a delayed onset of ice and an earlier breakup (Wang et al., 2018). This would increase the likelihood that storm waves occur when ice is either not present or when the NIC is not fully developed. Even if ice is present, thinner ice or less spatially extensive ice is not likely to provide the protective buffer that more expansive ice confers, thus erosion and associated sediment transport may be enhanced in the shallow portions of the nearshore. Given the uncertainties in these processes it is important to develop a better understanding of the morphodynamics associated with shore ice and to establish a method for predicting potential geomorphic impacts from variable ice scenarios.

We present here a combined field, laboratory, and modeling study that explores geomorphic change and sediment transport pathways related to winter shore ice. The aim of this study is to describe the role of shore ice in cold climate coastal evolution, which to date is poorly constrained yet potentially a key geomorphic agent. Field measurements of geomorphic change were collected at an open-coast sandy beach along the southern shore of Lake Superior in the North American Great Lakes to quantify the impacts of shore ice on nearshore morphology and sediment transport both immediately after the ice season as well as after several months of quiet conditions following ice off (Fig. 2). These field measurements and associated hydrodynamic processes were then used to provide the boundary conditions for cryogenic wave tank experiments and numerical modeling.

2. Materials and methods

2.1. Field study-study area

The field component of this study focused on Chocolay Beach, which is a ~ 0.25 km long sandy beach and bluff site located along the southern Lake Superior shoreline. This site was an ideal candidate to study beach and nearshore morphodynamics as shore ice is prevalent during the winter (long-term average of 64% ice cover) (Wang et al., 2017) and it is an open-coast site that is exposed to large wave events during strong northerly winds. Water levels fluctuate on event, seasonal, annual, and decadal timescales within Lake Superior, however during this study, water level only varied by ~0.3 m.

2.2. Field study- surveys

Field surveys were conducted on August 8, 2020, November 4, 2020, December 16, 2020, February 18, 2021, March 30, 2021, and September 20, 2021. During all field excursions except February 2021, topography data were collected with a drone, bathymetry were collected with a remote-controlled catamaran, and swash and inner surf zone morphology were mapped with RTK-GPS wading surveys. Only drone topography data were collected in the February 2021 field excursion to map the ice morphology when the NIC was fully developed.

Drone flights with a DJI Phantom 4 Pro V2.0 small unoccupied aerial system (sUAS) were conducted over Chocolay beach to collect high-resolution ground imagery (ground sampling distance of 1.5 cm per pixel) that were utilized to derive a digital elevation model (DEM) of the subaerial site topography (shoreline landward to the sandy bluff). Immediately prior to the flight, approximately twelve 0.3 m by 0.3 m

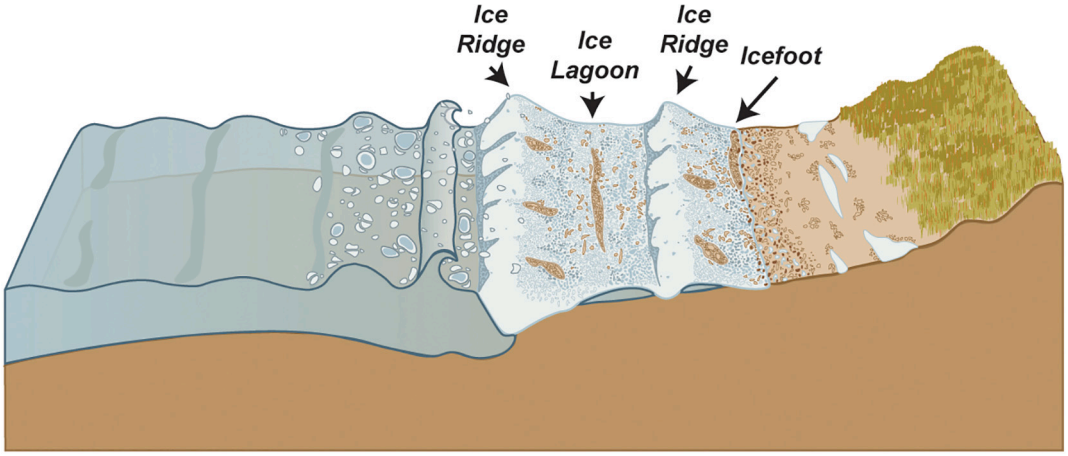

Fig. 1. Morphologic zones of the nearshore ice complex (NIC).

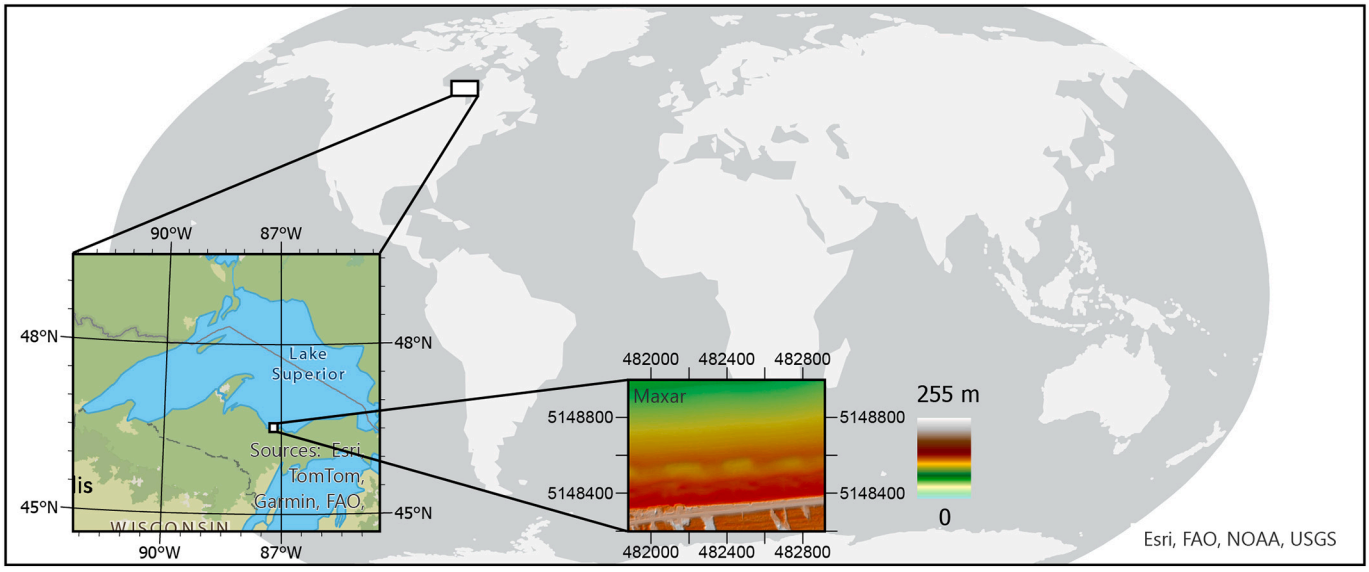

Fig. 2. Study area within Michigan, USA along the southern shore of Lake Superior. Left inset map depicts location of the study site within the Lake Superior region and the right inset map highlights the topobathymetric characteristics of the study site (elevation data downloaded from the National Oceanic and Atmospheric Administration's Data Access Viewer NOAA). The elevation data in this inset map are relative to the IGLD 85 vertical datum and the horizontal coordinates are in UTM (Zone 16 N; m).

black and white targets were placed throughout the subaerial portion of the site and surveyed with a Trimble R10–2 GNSS system as ground control points (GCPs) to spatially reference the drone imagery (horizontal and vertical precision ~3 cm). Drone-collected imagery were processed using structure-from-motion (SfM) photogrammetry implemented in Agisoft Metashape Professional. DEMs generated from SfM were exported as ASCII grid files with 0.5 m grid spacing and orthomosaic images were exported as TIFF files with pixel resolution of 0.05 m. Specific flight parameters and processing methods follow standard procedures outlined in Theuerkauf et al. (2021) and additional details are provided in the Supplemental Information for this manuscript.

A Seafloor Systems HyDrone remotely controlled catamaran equipped with a Seafloor Systems SonarMite single beam echosounder and a Trimble R10–2 GNSS system was deployed during calm wave conditions to collect bathymetric data (i.e., lakebed elevation) throughout the study site. Bathymetric data were collected primarily along shore-normal transects, however some additional data were gathered along parallel lines to minimize gridding artifacts. The catamaran could only resolve depths greater than 0.5 m therefore there was a gap in the shallow nearshore between the coverage from the sonar survey and the drone survey, which was filled with a RTK-GPS wading survey. The GNSS antenna was mounted on a 2.0 m pole and wading surveys were conducted along shore normal transects spaced approximately ~15 m apart. Wading surveys began at the shoreline and proceeded lakeward to wading depth (approximately 1 m water depth).

The wading and bathymetric survey data were then combined with the XYZ data from the drone DEM and then gridded in Surfer using the Natural Neighbor algorithm. The result was a seamless topobathymetric map with 5 m grid spacing. These topobathymetric maps were clipped to the size of the smallest mapped area and then Golden Software's Surfer program was used to subtract them from each other to derive DEMS of Difference (DODs). In these DOD maps, red colors denote erosion, white represents little to no change, and blue represents accretion.

2.3. Field study-hydrodynamics

Wave and water level data were gathered to document the hydrodynamic processes at the study site during the monitoring period from August 8, 2020 through September 20, 2021. Hourly water level data were gathered from NOAA for the Marquette Coast Guard Station (Station ID: 9099018; NOAA Tides and Currents). This station is approximately 13 km NW of the study site. These data were converted from the International Great Lakes Datum of 1985 (IGLD85) to the North American Vertical Datum of 1988 (NAVD88) by subtracting 0.0173 m to place the water level data into the same vertical datum as the topobathymetric data collected in this study. This conversion factor was established using the hydraulic corrector model for IGLD85 provided by the National Geodetic Survey.

Hourly significant wave height data were acquired from the Great Lakes Coastal Forecasting System (GLCFS) from the NOAA Great Lakes Environmental Research Laboratory (GLERL). The wave and water level data were divided into time periods defined by the field surveys and then analyzed to document the physical conditions associated with the geomorphic changes and establish the conditions that would be simulated in the wave tank and numerical model.

2.4. Field study-shore ice position

Satellite imagery products were collected from Planet using Planet Explorer to map the lakeward extent of shore ice during the winter ice season at the study site (Planet Team, 2017). Planet uses hundreds of Dove CubeSat satellites to collect daily imagery of Earth. This imagery was sourced through 4-band PlanetScope Scene at 3-m pixel resolution and ground sample distance of approximately 4 m. Thirteen cloud-free images were downloaded from mid-January 2021 to the end of March 2021 and the lakeward extent of the NIC was digitized in ArcMap 10.3. Shapefiles were generated from these digitized ice lines and used to evaluate spatial relationships between ice extent and documented geomorphic changes.

2.5. Wave tank experiments- tank details

To simulate observed field processes in a controllable and continually observable setting, a 3 m long × 0.6 m wide × 1.2 m tall wave tank was constructed in a large walk-in freezer of transparent acrylic with the capability of simulating the effects of shore ice and debris inclusion in ice through wave action (Theuerkauf et al., 2023; Dodge et al., 2024). Wave generating and temperature control methods are detailed in

Theuerkauf et al. (2023) and Dodge et al. (2024) (see Supplementary Material). The atmospheric temperature in the freezer was held at −6 °C to initiate ice formation at the water surface. The wave generator produced scaled waves similar to those recorded at different sites along the Great Lakes, but also extended the range of wave properties beyond those observed in the field to investigate a wider range of potential conditions. On the opposite side of the tank from the wave generator, a sediment bench with two adjustable ramps, a backshore ramp and a shoreface ramp meant to represent different coastal slopes, was installed to simulate beach, nearshore, and offshore environments. The slope of the backshore ramp was set at 20°. This was installed to create the backshore dune environment. By extending the backshore region, waves were able to extend up the beach face, simulating real world beach conditions. The shoreface ramp angle and position was held constant throughout all four experiments, set at ~5° angle, and the water height in the wave tank was adjusted so that the shoreface ramp represented an offshore environment. Sediment was placed on the sediment bench, creating a flat, ~ 2° slope, representing the nearshore and was piled up higher in the back end of the bench to represent offshore dunes. The sediment layer was sufficiently thick so that waves did not interact with the base material of the ramp. This 2° slope was similar to the shoreface slope at our field site of 3°.

2.6. Wave tank experiments-scaling and instrumentation

Following previous experiments in the same cryogenic wave tank (Theuerkauf et al., 2023; Dodge et al., 2024), experimental wavelength and period were scaled using Froude scaling to simulate deep water waves (Noble et al., 2017) (see supplemental material). Unlike previous cryogenic wave tank experiments (Theuerkauf et al., 2023; Dodge et al., 2024) the current study required sediment transport scaling. To accomplish sediment transport similitude the sediment used for the experiments was scaled using a non-dimensional Shields number (Dean and Dalrymple, 2004) to achieve similitude of sediment transport between the field site and the wave tank. A model achieves similitude when the model and real application share geometric, kinematic and dynamic similarity. The nondimensional Shields scaling, τ^* was estimated for both the wave tank and field and set equal to one another to achieve similitude.

$$\tau^* = \frac{\tau}{(\rho_s - \rho_l)gD_{50}} \tag{1}$$

$$\tau = \frac{1}{2} f U^2 \tag{2}$$

$$U = \frac{\pi 2a}{\mathrm{T}\ sinh(k^*h)} \tag{3}$$

Where ρ_s is the density of the sediment, ρ_l is the density of the liquid, g is the gravitational constant, D_{50} is the mean grain size diameter, and τ is the basal shear stress. The basal shear stress depends on f the frictional coefficient between the waves and bed material, and U the horizontal velocity. The horizontal velocity depends on a, the amplitude of the waves, h, the depth of the water and k, the wave number which is equal to $2\pi/L$, where L is the wavelength. Grain size analysis of samples from a similar Lake Superior beach to our study site (Bayview Beach, WI) were used for scaling and had a mean grain size of 788.5 μm and a density of 2.65 g/cm^3. To achieve similitude through Shields scaling, τ^*, we used a less dense scaled sediment with similar grain size to our Bayview Beach sand sediment. A coal slag blast media with a density of 1.3–1.7 g/cm^3 and a grain size of 710–850 μm was used in the wave tank to achieve similitude.

Experiments that were run until steady state did not require time to be scaled (e.g., Dodge et al., 2024), however, for the experiment where wave parameters varied with time (and steady state beach morphology may not be obtained) time scaling is a necessary factor. However, established scaling of time is less agreed upon than wave and sediment scaling. One study set their morphological time scale (n_{TM}) to the square root of their depth scale (n_h) (Van Rijn et al., 2011). The scaling ratio employed by the Army Corp of Engineers for the San Francisco Bay Model, scales time with the water depth ratio between the laboratory and the field, λ, and we have opted to utilize this same scaling relationship for our experiment. The ratio of water depth between the wave tank and the field is 1/46.5, hence roughly 1 h in the wave tank represents roughly 48 h in the field.

Multiple cameras were used to record visual observations of the ice and sediment movement throughout the experiments. An underwater camera tracked the motion of sediment and wave propagation below the ice cap. An aerial camera tracked nearshore bar movement as well as ice growth and retreat. A horizontal camera placed along the sediment bench captured nearshore bar movement and sediment transport beyond the depth of closure. Images were captured every minute and timelapse videos were created using LabView Software and Microsoft Video Editor. Additionally, the beach face morphology was documented following the completion of the experiments through structure-from-motion techniques (detailed previously).

2.7. Wave tank experiments-experiment parameters

A total of two experiments were performed within the wave tank both using the less dense scaled coal sediment (see videos of experiments in Supplementary Materials). The first experiment examined sediment transport under constant wave conditions during the formation of the NIC whereas the second experiment examined the effect of variable wave conditions on sediment transport during the formation of the NIC. In the first experiment the waves had a constant wavelength and amplitude. The freezer temperature was set to −6 °C, the wave generator produced waves of a wavelength and amplitude of ~0.5 m and 0.01 m, respectively. The water depth within the wave tank was 0.43 m. Once a NIC had formed, the ice was melted, and the water drained from the wave tank. Images from various angles were taken of the bed, before and after the experiment, for use in structure from motion to observe how sediment had been mobilized. The second experiment was also performed using the scaled coal sediment, the scaled time factor, and variable wave conditions. The scaling relationship used for this wave tank experiment was based off a GLERL wave model projected for ~20 m water depth, collected from the Marquette, MI site from 12/12/2020 to 03/30/2021. Field wave conditions were simplified into two groups, quiet conditions (e.g., low wave amplitude and short period), with a wave period and amplitude of 3 s and 0.25 m, respectively and wavy conditions (e.g., moderate wave amplitude and a longer period), with a wave period and amplitude of 5 s and > 0.5 m, respectively. Within the scaled wave tank experiment, a wavelength and height of ~0.3 m and ~ 0.01 m, respectively, was produced for the quiet conditions and a wavelength and height of ~0.8 m and ~ 0.02 m, respectively, was produced for the wavy conditions. Using this scaling for the experiment the time scale was simplified to ~10 h of quiet conditions and ~ 2.5 h for wavy conditions. These wave conditions were held until initial shore ice formed. At this point, waves were produced with a wavelength and amplitude of ~0.3 m and ~ 0.01 m, respectively, to simulate quiet conditions recorded in the field. These wave conditions were held for ~10 h. After this time, we resumed wavy conditions for ~2.5 h. We repeated this time sequence of ~10 h of quiet conditions and ~ 2.5 h of wavy conditions until a NIC fully formed.

2.8. Numerical modeling

XBeach is an open-source, process-based model originally formulated for simulating hydro- and morphodynamics of extreme storm events on the scale of kilometers (Roelvink et al., 2009). The applications of XBeach have since been expanded and validated for a wider range of coastal environments and processes. XBeach solves the wave

action balance to acquire the wave forcing, while flows and sediment transport are calculated through depth-averaged shallow water and advection-diffusion equations respectively. (For more details see the XBeach User Manual; Roelvink et al., 2010). For this study, we applied a short-wave averaged, long-wave resolving hydrodynamic formulation (Surfbeat) to focus computational power on the infragravity waves that dominate during storm episodes. All other parameters were left at the default values for the version used, which was XBeach 1.24.6057 "Halloween".

We created a computational grid based on the 5 m resolution bathymetry data collected on 12/16/2020 using the OpenEarth XBeach toolbox for Matlab (https://github.com/openearth). The ice positions from 01/03/2021 and 01/30/2021 as mapped from the Planet satellite data were used because they represent, respectively, the conditions preceding the first significant wave activity and a maximum ice extent before storm conditions (wave height above 1.5 m) that fell entirely within the survey area. Grid cells corresponding to nearshore ice were designated as a non-erodible structure and given an elevation value of 0.5 m above starting mean water level. Wave data were obtained from the POM-based GLCFS model for Lake Superior (https://www.glerl.noaa.gov/res/glcfs/) and filtered to get a timeseries of significant wave heights above 1.5 m. These wave conditions were used to drive the 2D simulation for 100 storm hours between 1/22/2021 and 3/29/2021. A majority (>95 %) of the storm waves approached the site from the north, and were modelled as approaching normal to the coast. The final model bathymetry was interpolated back to the 5 m resolution survey grid using a Nearest Neighbor technique in Matlab. Roller energy dissipation, which is representative of transformation of incoming waves (Streßer et al., 2022) was calculated across the model domain as a proxy for wave breaking.

3. Results and interpretations

3.1. Field observations

Repeat topobathymetric surveys at the Lake Superior site reveal that the presence of shore ice was associated with substantial nearshore geomorphic change (Fig. 3). Following ice off, in the nearshore proximal to the shoreline, deposition was documented while lakebed erosion was observed further lakeward. Deposition near the shoreline was located just landward of the average ice extent mapped from satellite imagery (Fig. 4). The position of the lakeward ice ridge position aligns spatially with the pre-ice (December 2021) location of the bar and trough system, which developed in response to storms and subsequent recovery during the fall of 2020.

Lakeward of the NIC, a large zone of scour (~100 m in width and ~ 1 m in depth) was documented in the post-ice topobathymetric survey (Fig. 3). A small zone of deposition was also observed immediately lakeward of the ice extent on the western end of the site. This depositional area occurs immediately lakeward of an embayed portion of the NIC edge (Fig. 3), which may have created a depositional hotspot for the scoured material or other material moving in the littoral drift. Overall, the results from the pre- and post-ice mapping reveal that there was a clear linkage between the pre-ice morphology, the geometry of the NIC, and the immediate post-ice geomorphic impacts yet the temporal persistence of these impacts also needed to be evaluated.

The site was mapped again in September 2021 to determine whether the geomorphic impacts of the shore ice persisted throughout the year (Fig. 3). The dominant response throughout the site during the period from March 2021 through September 2021 was erosion. There was some deposition documented in the scour zone, however most of this area continued to erode. Upper shoreface and swash zone erosion was observed at the eastern end of the site. It appears that most of the

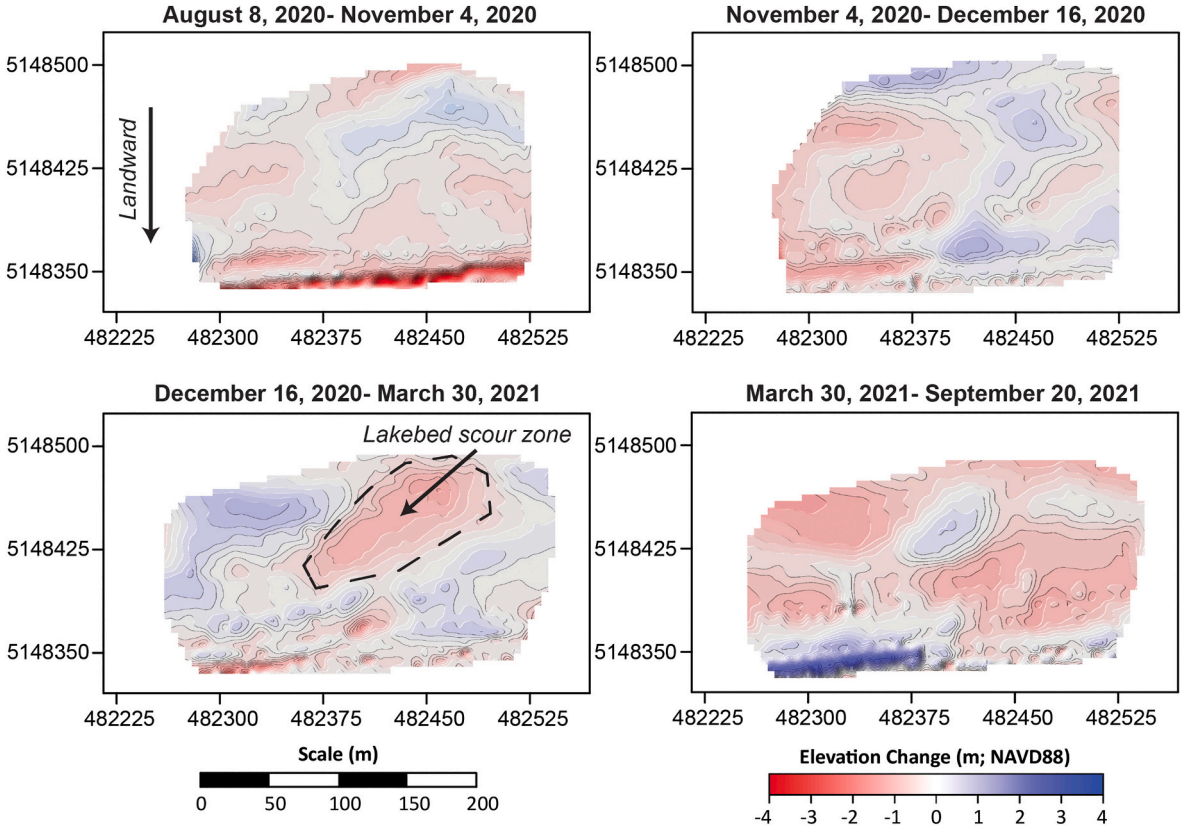

Fig. 3. Chocolay Beach DEMs of Difference generated from field surveys. Note the area of lakebed scour in the December 16, 2020 to March 30, 2021 generated by wave breaking along the lakeward extent of the NIC.

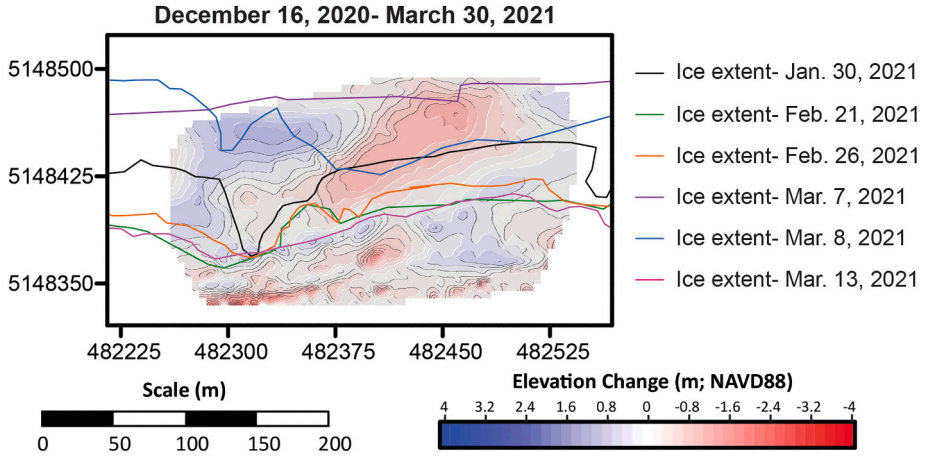

Fig. 4. Satellite-derived lakeward NIC extent lines compared to the net beach and nearshore morphology change during the winter of 2021. The lakebed scour zone generally corresponds with the area just lakeward of the NIC. The bottom of the figure is shoreward and the top is lakeward.

material that was deposited adjacent to the shoreline during decay of the ice ridge/icefoot was removed during the period from March to September. No major storms were documented during this time that could explain the pervasive erosion. A large area of subaerial accretion on the southwestern end of the site is the result of a rock revetment that was installed in summer 2021 and was not related to any ice-associated geomorphic pattern. Overall, it appears that much of the upper shoreface geomorphic change resulting from the presence of shore ice is ephemeral as material that was eroded and deposited is reworked during the following period; however, deeper nearshore scour in front of the NIC persisted even after other portions of the lakebed adjusted after ice-off.

3.2. *Experimental simulations*

Whereas the topobathymetric mapping results provided new insight on the short and longer-term impacts of shore ice they did not allow for real-time observation of sediment transport that could provide insight into the dominate NIC related processes, but the wave tank observations provided insights to the causes of change. Initially, as the temperature of the water in the wave tank approached freezing an icefoot formed along the beach. During periods of increased wave energy, the NIC grew basinward and the ridges that formed were spatially associated with a sandbar (Fig. 5; Supplementary Materials). Sediment transported on the lakebed immediately in front of the NIC was highly dynamic and the bar can be seen migrating onshore and offshore as the NIC position changes.

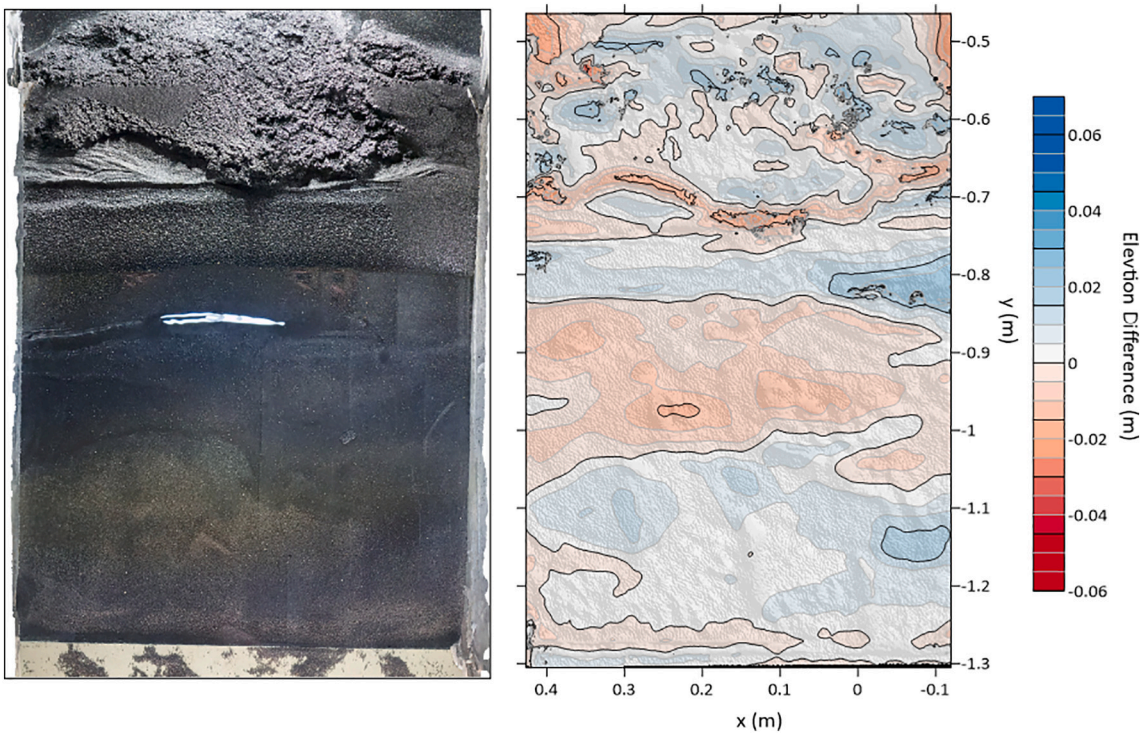

Fig. 5. Summary graphic from wave tank experiment. The figure on the right shows a DOD from the wave tank experiment 2 with erosion in red and deposition in blue. The water line was near −0.8 on the vertical axis and all values below one on the vertical axis were below the water level. The plot shows erosion in the nearshore where the NIC existed and deposition in deeper waters in response to scour at the base of the NIC. Note creation of a similar DOD for experiment 1 was not possible due to insufficient images from before the wave action.

As the NIC continues to migrate lakeward, it appears to reach a threshold position on the shoreface where bed scour is initiated. Once this scour begins the sediment is rapidly transported offshore into deeper water. In the wave tank simulation, no onshore transport of this scoured sediment was observed under ice free conditions with the same waves, indicating the presence of the NIC caused erosion and deposition in portions of the bed that would have otherwise been unaffected. Fig. 5 shows scour (red) outboard of the NIC ridge near −0.9 to −1.1 while the upper shoreface was largely protected (blue) by the nearshore ice near −0.8.

3.3. Numerical modeling

The combination of the wave tank simulations and the field observations highlights the geomorphic processes and responses associated with shore ice. To further explore these processes we used the numerical model XBeach to simulate the sediment transport and the geomorphic response of the nearshore to ice of different extents. The model outputs revealed a spatial pattern of erosion and accretion that was consistent with what was documented in the pre and post ice topobathymetric maps, but with lower magnitudes given the shorter duration and singular (non-moving) ice extents of the model run compared to the full ice on season. For both model runs scour was observed just lakeward of the shore ice and deposition was documented immediately along the ice ridge (Fig. 6). Both model runs captured the pattern of scour in the northeast-central survey area. The concentrated deposition observed from the survey in the northwest zone of the site was only replicated for the greater ice extent (01/31/2021; Fig. 6). This model run also better simulated the accretion just west of the scour zone, which was one of the dominant responses documented in the survey data and likely results from longshore transport of the scoured nearshore sediment. Although it is difficult to represent varying ice extents in a single model, these two stationary ice extents show that ice will have a unique morphologic signature on the nearshore for each extent. Since the model only simulated storm events (significant wave height >1.5 m), these data show the storm-condition dependence of the lakebed scour adjacent to the ice. To corroborate these morphologic impacts with a physical process, we computed the average roller energy dissipation for the full timeseries (Fig. 7). The roller dissipation shows that a small amount of dissipation occurs over the furthest offshore bar located at a cross-shore distance of 250 m, but most of the energy is dissipated at the ice margin (Fig. 7).

4. Discussion

In contrast to previous studies that assert that either erosion or accretion occur in response to the presence of ice, both accretion and erosion were observed in our post-ice surveys; however, there was a structured spatial variability in these responses that differed from expectations. It appears that the scour zone was spatially related to the location of the ice complex throughout the winter, which as our model and wave tank data show, was likely a function of both the hydrodynamics (wave conditions building the ridges) and the nearshore

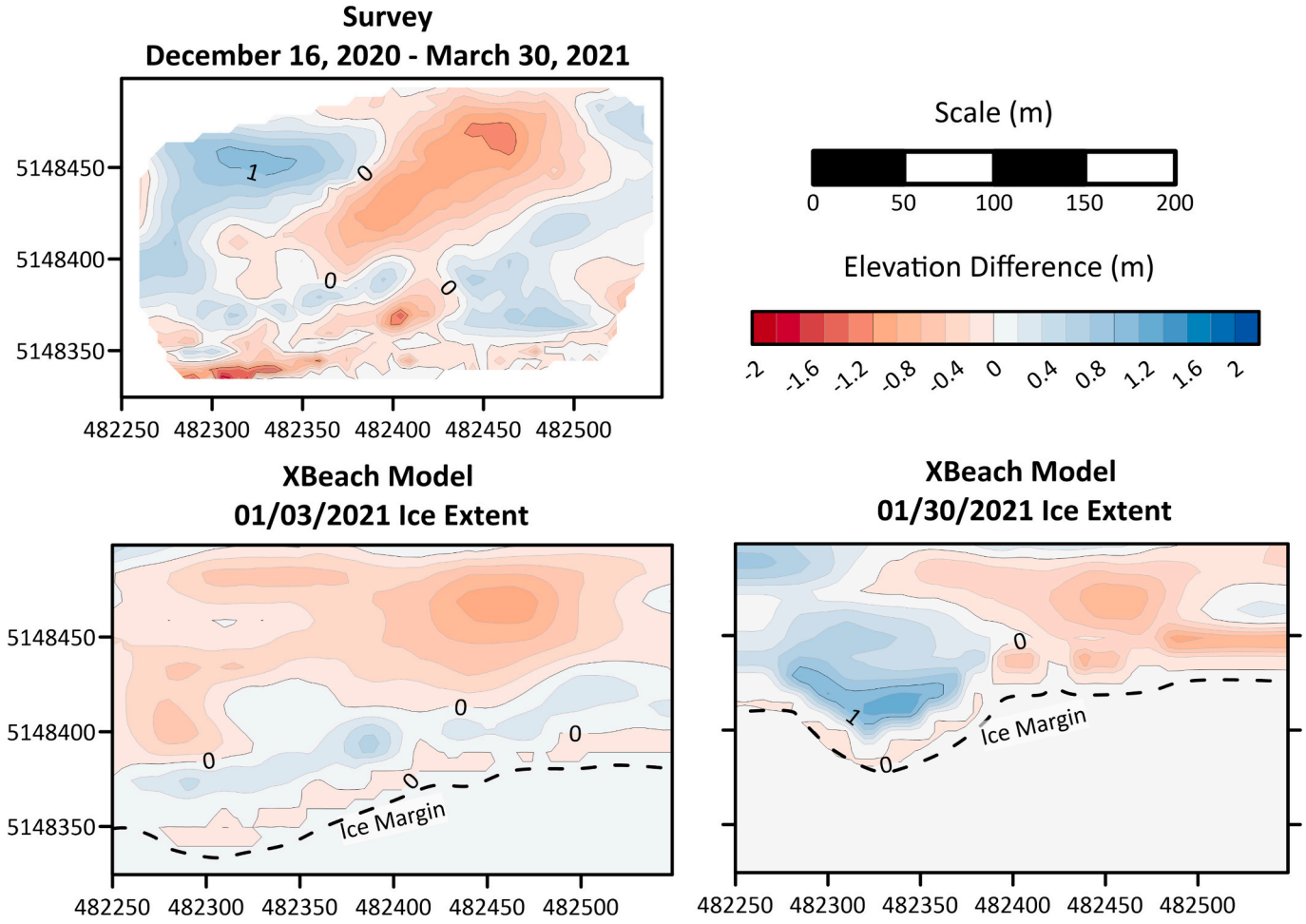

Fig. 6. Summary graphic from field survey data (top left) compared to the modeling output (bottom). Models use the same forcing conditions but different ice extents. The models capture a general pattern of scour immediately basinward of the ice ridge and deposition basinward of the ridges. Scour is likely greater in the field data than the modeling data due to the spatial variability in ice presence throughout the winter, which varies the location of scour or deposition.

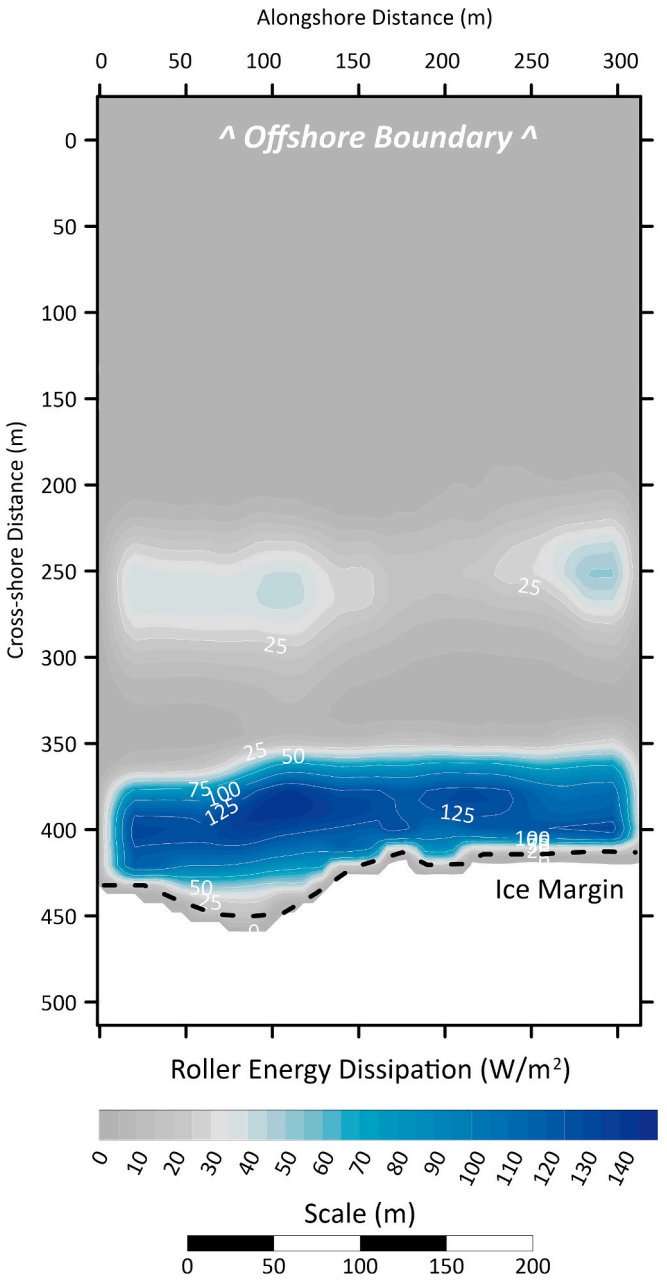

Fig. 7. A map of the model domain showing total roller energy dissipation averaged over the timeseries of the model. Higher values of average roller energy dissipation suggest stronger wave transformation and generation of turbulence.

bathymetry. The position of the ridges aligns spatially with the location of the bar and trough system that developed in response to storms and subsequent recovery during the fall of 2020. The deposition near the shoreline appears to be primarily the result of in-place melting of the ice ridge and icefoot and the subsequent deposition of debris entrained with in the ice given its location just landward of the average ice extent mapped from satellite imagery.

Both the scour and the deposition are attributed to waves breaking along the lakeward edge of the NIC, scouring the bed and transporting lakebed sediments lakeward. As waves impinge upon the NIC, their energy is deflected downward into the lakebed resulting in scour similar to the effects of sea walls. The spatial distribution of roller energy dissipation supports the notion of wave transformation and turbulence generation at the icefront. A similar pattern of erosion and deposition has been documented in past studies (e.g. Barnes et al., 1993; Bajorunas and Duane, 1967), but the scour zone observed in this study has a much larger spatial footprint than previous studies (~100 m vs 1 m in width) and is substantially deeper (~1 m vs centimeters). The larger spatial extent of the scour is likely attributed to changes in the NIC position throughout the winter season and the ability to survey greater areas with the remotely controlled sonar vehicle. As the lakeward extent of the NIC expands and recedes the location of the scour also changes (Fig. 6) resulting in beveling of the lakebed (Fig. 4). Our post-ice top-obathymetric mapping was able to capture the net effect of this process.

We attribute the sustained beach and upper shoreface erosion after ice off (March 2021 through September 2021) to the down cut lakebed that resulted from the icefront scour. Since wave energy was generally low during this period, waves did not break until they reached the shallower portions of the shoreface close to shore. This likely resulted in erosion of these areas during periods when minimal erosion and perhaps accretion would be anticipated. Although much of the nearshore bathymetry was returned to the pre-ice (August 2020) morphology in response to sediment redistribution during this time, a substantial portion of the scour zone persisted.

The temporal persistence of the geomorphic impacts of the NIC has not been documented before, and the affects appear to have a long-lasting impact on the nearshore sediment budget through eroding and depositing sediments in areas that would have likely remained unaffected if it were not for the presence of the NIC. While these field data allowed us to document the net effect of the shore ice on the morphology, our ability to fully capture processes and responses was limited by these snapshots. The wave tank and modeling experiments conducted in this study provided a temporally continuous record of the sediment transport processes that likely occurred in-situ at the study site. These allowed us to observe in more detail how shore ice modulates morphodynamic processes and provided insights that extend our understanding of the fundamental geomorphic change mechanisms along cold climate coasts.

The wave tank experiments revealed that the NIC was spatially related to a sandbar that formed along the nearshore and that as the NIC grew, scour and sediment transport were most active at the basinward extent of the ice. As the NIC extended further into the basin, it ultimately reached a point where the scoured sediment began to be transported offshore, towards the depth of closure (Supplementary Materials). From this, one of the potential geomorphic impacts of shore ice is to transport shoreface sediments basinward past the depth of closure, which could essentially remove them from the nearshore sediment budget. At this time, no sediment budgets are accounting for this loss term, which depending on the site could be substantial. The removal of this sand from the nearshore budget could limit beach recovery and in some cases, such as was observed in the field data from this study, enhance non-storm erosion.

The model data suggests that the bed scour and associated nearshore sediment transport is likely event driven rather than a continuous process throughout the winter. When wave energy approaches the NIC, particularly during storms, the energy dissipation (Fig. 7) suggests the waves are transformed and turbulence is deflected towards the bed resulting in scour. As the NIC position migrates across the shoreface throughout the winter in response to changing meteorologic and hydrodynamic conditions, the location of wave energy impact and morphologic change on the bed also varies (Fig. 6). The net effect of multiple storm events occurring throughout the winter is to lower the shoreface elevation, which depending on the magnitude can be persistent even after ice-off and/or sediment deposition from longshore currents or bar migration. Declining sea ice in other cold climate regions, such as the Arctic, have been related to similarly high spatiotemporal complexity in coastal geomorphic response, thus supporting the notion that future models and management plans should consider the impacts of declining and dynamic shore ice (e.g., Overeem et al., 2011; Farquharson et al., 2018; Nielsen et al., 2022).

Given the spatial relationship between the NIC position and bed changes (i.e., nearshore sediment transport) documented through the field and wave tank observations and modeling experiments we propose that the general location of shoreface erosion associated with winter shore ice can be predicted by identifying the NIC position on the shoreface during high energy wave events. Based on the findings from previous studies (e.g. Barnes et al., 1993; Bajorunas and Duane, 1967) and our study, scour is likely just basinward of the NIC during these events and therefore can be probabilistically mapped through time. Satellite or drone-based imagery can be used to discern the location of the NIC at any given point in time and then mapped onto the pre-ice bathymetry. Once these positions are mapped, it can be inferred that if a large wave event occurs while the NIC is in that position scour will occur basinward of the NIC. Probable areas of this scour could be mapped onto the pre-ice bathymetry and used to predict bed changes throughout the winter season. These predictions should be validated against post-ice bathymetry to determine the accuracy of this method for forecasting geomorphic changes related to shore ice at a given location.

If the NIC position varies substantially throughout the winter and numerous storm wave events occur it can be inferred that a scour zone, such as the one documented in this study, will form, which could lead to changes in the nearshore sediment budget as sediment may be transported past the depth of closure. This probabilistic approach could be used by coastal practitioners who are interested in identifying potential changes to the nearshore morphology and/or sediment budget but are not able to gather high resolution bathymetric data or run numerical models. This approach is particularly relevant for Arctic locations and other remote cold climate coastlines where field data collection may be challenging but there is a need to understand potential for shore ice-related geomorphic impacts.

5. Conclusions

The first ever combined field, laboratory, and modeling study of the geomorphic impacts of shore ice revealed that ice can simultaneously enhance nearshore erosion and protect the beach from erosion (directly when ice is present and subsequently via deposition of entrained sediment during breakup). This contrasts previous work which suggest that at a given location ice either has a protective or erosional influence. From our field results, scouring at the basinward edge of the ice leads to substantial areas of bed erosion that influence wave breaking during following periods. Enhanced erosion during calm weather conditions was observed in these areas where a deepened bed forced waves to break at or near the shoreline. These field observations were substantiated during both cryogenic wave tank and numerical modeling experiments. Wave tank experiments reveal that not only can ice lead to nearshore scour, but also offshore directed sediment transport which can remove material from the nearshore sediment budget. Numerical modeling simulations defined the physical mechanisms that lead to enhanced bed scour during shore ice presence and further documented the sediment transport pathways associated with shore ice. Our findings suggest that shore ice plays a direct role in eroding the nearshore and an indirect role in facilitating beach and upper shoreface erosion even during calm, non-ice conditions. Given these dynamics, shore ice should be incorporated into coastal geomorphic evolution models along cold-climate coastlines and must be considered an important agent of change for coastal management.

Funding

Funding support for this project was provided by the National Science Foundation through awards to E.J. Theuerkauf (1950101) and L.K. Zoet (1916179).

Open research

All data from this study are maintained on Michigan State University and University of Wisconsin-Madison servers and can be supplied to interested individuals by written request to the corresponding author.

CRediT authorship contribution statement

E.J. Theuerkauf: Writing – original draft, Visualization, Validation, Supervision, Software, Resources, Project administration, Methodology, Investigation, Funding acquisition, Formal analysis, Data curation, Conceptualization. **L.K. Zoet:** Writing – review & editing, Visualization, Validation, Supervision, Software, Resources, Project administration, Methodology, Investigation, Funding acquisition, Formal analysis, Data curation, Conceptualization. **C.A. Volpano:** Writing – review & editing, Visualization, Validation, Methodology, Investigation, Formal analysis. **S.E. Dodge:** Visualization, Validation, Methodology, Investigation, Formal analysis. **B.M. Hartley:** Visualization, Methodology, Investigation, Formal analysis. **J. Elmo Rawling:** Writing – review & editing, Supervision, Project administration, Investigation, Funding acquisition.

Declaration of competing interest

The authors declare that they have no known competing financial interests or personal relationships that could have appeared to influence the work reported in this paper.

Data availability

Data will be made available on request.

Acknowledgments

The authors would like to thank Lucas Rabins, Sarah Grace Lott, and Ryan Poe for field and laboratory assistance with the geomorphic mapping component of the study. Additionally, the authors would like to thank Peter Sobol for assistance with the wave tank construction and Mary DeBona for assistance in the creation of Fig. 1.

Appendix A. Supplementary data

Supplementary data to this article can be found online at https://doi.org/10.1016/j.geomorph.2024.109409.

References

Bajorunas, L., Duane, D.B., 1967. Shifting offshore bars and harbor shoaling. J. Geophys. Res. 72 (24), 6195–6205. https://doi.org/10.1029/JZ072i024p06195.

BaMasoud, A., Byrne, M.-L., 2012. The impact of low ice cover on shoreline recession: a case study from Western Point Pelee, Canada. Geomorphology 173–174, 141–148. https://doi.org/10.1016/j.geomorph.2012.06.004.

Barnes, P.W., Kempema, E.W., Reimnitz, E., McCormick, M., 1994. The Influence of Ice on Southern Lake Michigan Coastal Erosion. J. Great Lakes Res. 20 (1), 179–195. https://doi.org/10.1016/S0380-1330(94)71139-4.

Barnes, P.W., Kempema, E.W., Reimnitz, E., McCormick, M., Weber, W.S., Hayden, E.C., 1993. Beach Profile Modification and Sediment Transport by Ice: an Overlooked Process on Lake Michigan. J. Coast. Res. 9 (1), 65–86.

Brady, M.B., Leichenko, R., 2020. The impacts of coastal erosion on Alaska's North Slope communities: a co-production assessment of land use damages and risks. Polar Geogr. 43 (4), 259–279. https://doi.org/10.1080/1088937X.2020.1755907.

Bryan, M.L., Marcus, M.G., 1972. Physical Characteristics of Near-Shore Ice Ridges. ARCTIC 25 (3), 182–192. https://doi.org/10.14430/arctic2960.

Dean, R.G., Dalrymple, R.A., 2004. Coastal Processes with Engineering Applications.

Dodge, S.E., Zoet, L.K., Rawling, J.E., Morgan-Witts, N., Theuerkauf, E.J., 2024. The effects of beach energy on sediment entrainment within the nearshore ice complex. J. Great Lakes Res. 102379 https://doi.org/10.1016/j.jglr.2024.102379.

Dodge, S.E., Zoet, L.K., Rawling, J.E., Theuerkauf, E.J., Hansen, D.D., 2022. Transport properties of fast ice within the nearshore. Coast. Eng. 177, 104176 https://doi.org/10.1016/j.coastaleng.2022.104176.

Evenson, E.B., Cohn, B.P., 1979. The ice-foot complex; its morphology, formation and role in sediment transport and shoreline protection. Zeitschrijt Fur Geomorphologie 23, 58–75.

Farquharson, L.M., Mann, D.H., Swanson, D.K., Jones, B.M., Buzard, R.M., Jordan, J.W., 2018. Temporal and spatial variability in coastline response to declining sea-ice in Northwest Alaska. Mar. Geol. 404, 71–83. https://doi.org/10.1016/j.margeo.2018.07.007.

Forbes, D.L., Taylor, R.B., 1994. Ice in the shore zone and the geomorphology of cold coasts. Progress in Physical Geography: Earth and Environment 18 (1), 59–89. https://doi.org/10.1177/030913339401800104.

Kempema, E.W., Reimnitz, E., Barnes, P.W., 2001. Anchor-Ice Formation and Ice Rafting in Southwestern Lake Michigan, U.S.a. J. Sediment. Res. 71 (3), 346–354. https://doi.org/10.1306/2DC40948-0E47-11D7-8643000102C1865D.

Manson, G.K., Davidson-Arnott, R.G.D., Ollerhead, J., 2015. Attenuation of Wave Energy by Nearshore Sea Ice: Prince Edward Island. Canada. Journal of Coastal Research 32 (2), 253. https://doi.org/10.2112/JCOASTRES-D-14-00207.1.

Marsh, W.M., Marsh, B.D., Dozier, J., 1973. Formation, structure, and geomorphic influence of Lake Superior icefoots. Am. J. Sci. 273 (1), 48–64. https://doi.org/10.2475/ajs.273.1.48.

McCann, S.B., Taylor, R.B., 1975. Beach Freezeup Sequence at Radstock Bay, Devon Island. Arctic Canada. Arctic and Alpine Research 7 (4), 379–386. https://doi.org/10.1080/00040851.1975.12003848.

Miner, J.J., Powell, R.D., 1991. An Evaluation of Ice-Rafted Erosion Caused by an Icefoot complex, Southwestern Lake Michigan, U.S.a. Arct. Alp. Res. 23 (3), 320–327. https://doi.org/10.1080/00040851.1991.12002851.

Nielsen, D.M., Pieper, P., Barkhordarian, A., Overduin, P., Ilyina, T., Brovkin, V., Baehr, J., Dobrynin, M., 2022. Increase in Arctic coastal erosion and its sensitivity to warming in the twenty-first century. Nat. Clim. Chang. 12, 263–270. https://doi.org/10.1038/s41558-022-01281-0.

Noble, D.R., Draycott, S., Davey, T.A.D., Bruce, T., 2017. Design diagrams for wavelength discrepancy in tank testing with inconsistently scaled intermediate water depth. Int J Mar Energy 18, 109–113.

Overeem, I., Anderson, R.S., Wobus, C.W., Clow, G.D., Urban, F.E., Matell, N., 2011. Sea ice loss enhances wave action at the Arctic coast. Geophys. Res. Lett. 38 https://doi.org/10.1029/2011GL048681.

Planet Team, 2017. Planet Application Program Interface. In Space for Life on Earth, San Francisco, CA. https://api.planet.com.

Roelvink, D., Reniers, A., van Dongeren, A., van Thiel de Vries, J., McCall, R., & Lescinski, J., 2009. Modelling storm impacts on beaches, dunes and barrier islands. Coast. Eng. 56 (11), 1133–1152. https://doi.org/10.1016/j.coastaleng.2009.08.006.

Roelvink, D., Reniers, A., Van Dongeren, A. P., Van Thiel de Vries, J., Lescinski, J., & McCall, R. (2010). XBeach model description and manual. *Unesco-IHE Institute for Water Education, Deltares and Delft University of Tecnhology. Report June*, *21*, 2010.

Seibel, E., Carlson, C.T., Maresca, J.W., 1976. Ice Ridge Formation: Probable Control by Nearshore Bars. J. Great Lakes Res. 2 (2), 384–392. https://doi.org/10.1016/S0380-1330(76)72301-3.

Streßer, M., Horstmann, J., Baschek, B., 2022. Surface wave and roller dissipation observed with shore-based Doppler marine radar. J. Geophys. Res. Oceans 127, e2022JC018437.

Theuerkauf, E., Mattheus, C.R., Braun, K., Bueno, J., 2021. Patterns and processes of beach and foredune geomorphic change along a Great Lakes shoreline: Insights from a year-long drone mapping study along Lake Michigan. Shore & Beach 46–55. https://doi.org/10.34237/1008926.

Theuerkauf, E.J., Zoet, L.K., Dodge, S.E., Tuttle, W., Rawling III, J.E., 2023. Nearshore ice complex breakup is controlled by a balance between thermal and mechanical processes. Earth Surf. Process. Landf. 48 (15) https://doi.org/10.1002/esp.5698.

Van Rijn, L.C., Tonnon, P.K., Sánchez-Arcilla, A., Cáceres, I., Grüne, J., 2011. Scaling laws for beach and dune erosion processes. Coast. Eng. 58 (7), 623–636. https://doi.org/10.1016/j.coastaleng.2011.01.008.

Wang, J., Kessler, J., Bai, X., Clites, A., Lofgren, B., Assuncao, A., et al., 2018. Decadal Variability of Great Lakes Ice Cover in Response to AMO and PDO, 1963–2017. J. Clim. 31 (18), 7249–7268. https://doi.org/10.1175/JCLI-D-17-0283.1.

Wang, J., Kessler, J., Hang, F., Hu, H., Clites, A.H., Chu, P., 2017. Analysis of Great Lakes ice cover climatology: Winters 2012–2017. NOAA Tech. Memo. GLERL-171, 24. https://www.glerl.noaa.gov/pubs/tech_reports/glerl-171/tm-171.pdf.

Zimmermann, M., Erikson, L.H., Gibbs, A.E., Prescott, M.M., Escarzaga, S.M., Tweedie, C. E., et al., 2022. Nearshore bathymetric changes along the Alaska Beaufort Sea coast and possible physical drivers. Cont. Shelf Res. 242, 104745 https://doi.org/10.1016/j.csr.2022.104745.